A study on the exchange coupling of NdFeB-type nanocomposites using Henkel plots

Q. Chen and B. M. Ma[a)]
Rhodia Inc., Rare Earths and Gallium, CN 7500, Cranbury, New Jersey 08512

B. Lu, M. Q. Huang, and D. E. Laughlin
Department of Materials Science and Engineering, Carnegie Mellon University, Pittsburgh, Pennsylvania 15213

The phase transformation and magnetic properties of $(Nd_{0.95}La_{0.05})_{9.5}Fe_{bal}Co_5Nb_2B_{10.5}$ nanocomposite have been investigated systematically via thermomagnetic analysis, vibration sample magnetometer, x-ray diffraction, and conventional transmission electron microscopy. The Henkel plot was employed to quantify the strength of the exchange coupling between the hard and soft magnetic phases in the as-spun and the thermally treated samples. It was found that remanence B_r, coercivity H_{ci}, and maximum energy product BH_{max} obtained were affected by the magnetic phases present as well as the grain size of constituent phases and their distribution. The Henkel plot successfully interpreted the effect of the exchange coupling on B_r, H_{ci}, and BH_{max} obtained for samples treated below 750 °C. However, it became inadequate for samples treated above 750 °C. Although similar shapes of $\Delta M-H$ curves were obtained in the Henkel plot, severe degradation in B_r, H_{ci}, and BH_{max} was found when the thermal treatment temperature was increased from 750 to 850 °C. This degradation may be attributed to the grain growth of the main phases, from 45 to 68 nm, and the development of precipitates. In conjunction with the mass balance, the precipitated phases (presumably borides) may explain the increase in the T_c of $Nd_2(FeCo)_{14}B$ and the decreased amount of α-Fe and Fe_3B with increasing thermal processing temperature. © *1999 American Institute of Physics.* [S0021-8979(99)47508-5]

INTRODUCTION

Recently, NdFeB nanocomposite intermetallic compounds have attracted much attention in both the scientific community and bonded magnet industry.[1–5] Composed of both magnetically hard and soft phases, nanocomposites usually possess enhanced remanence due to the exchange coupling.[1–4] The overall magnetic performances, namely remanence B_r, coercivity H_{ci}, and maximum energy product $(BH)_{max}$ are dictated by the strength of the exchange coupling as well as by the magnetic phases present in the nanocomposites.

Using a three dimensional modeling, Schrefl *et al.*[4] estimated that the ideal grain size should be approximately 20 nm for the hard phases and 10 nm for the soft phases. Nanoscaled grain size can be achieved by optimal quenching or by overquenching followed by a crystallization treatment. It is generally recognized that an increase in the thermal processing temperature results in grain growth. The grain growth usually becomes more rapid at higher temperatures. An excessive grain growth may weaken the exchange coupling and lowers the overall magnetic performance of nanocomposites. However, the impact of the magnetic phase transformation using different thermal processing conditions on the exchange coupling and subsequent magnetic properties have not received the same attention.

Henkel plots have been widely used in the recording media to describe the interacting particle systems.[7–9] This technique can also provide a quantitative means to describe the exchange coupling in the newly developed nanocomposites for permanent magnets.[9] However, many features must be addressed to apply this technique correctly to describe the exchange coupling in the nanocomposites.

In this work, the effect of both the exchange coupling and the magnetic phases on the magnetic performances of a rare-earth-lean and boron-rich NdFeB nanocomposite, $(Nd_{0.95}La_{0.05})_{9.5}Fe_{bal}Co_5Nb_2B_{10.5}$, is reported. While the detailed microstructural work via the conventional transmission electron microscopy (CTEM) will be reported in a supporting article;[10] this study focuses on the characterization of exchange coupling via the Henkel plot, and the effect of the magnetic phases on B_r, H_{ci}, and $(BH)_{max}$.

EXPERIMENT

$(Nd_{0.95}La_{0.05})_{9.5}Fe_{bal}Co_5Nb_2B_{10.5}$ ribbons were prepared via the conventional melt-spinning technique. The as-melt-spun materials were isothermally treated in a tube furnace under vacuum at 650, 700, 750, and 850 °C. The magnetic properties at room temperature were measured by an EG&G Model 4500 vibration sample magnetometer (VSM) with a maximum applied magnetic field of 18 kOe. All samples were pulse magnetized at 100 kOe prior to each measurement. A Perkin–Elmer model 7 thermogravimetric analyzer (TGA) was modified to perform thermomagnetic analysis (TMA). An x-ray diffractometer (XRD) (Siemens) with Co radiation ($\lambda=1.788\,97$ Å) was used to determine the amorphocity of the as-spun materials.

a)Electronic mail:bma@us.rhodia.com

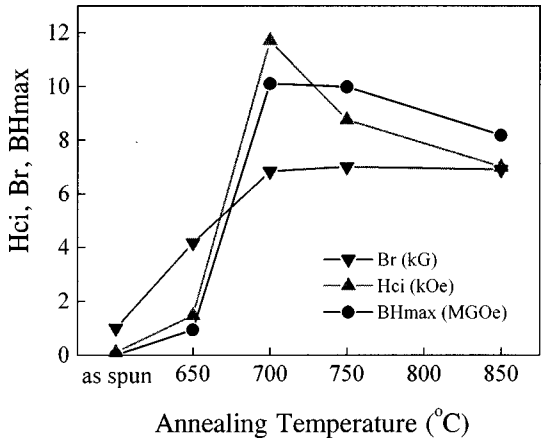

FIG. 1. Magnetic properties of as-melt-spun and thermally processed $(Nd_{0.95}La_{0.05})_{9.5}Fe_{bal}Co_5Nb_2B_{10.5}$.

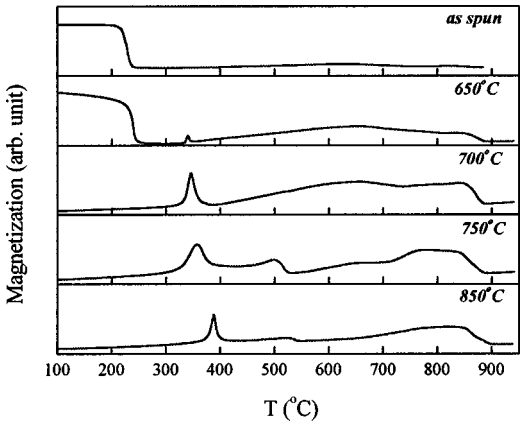

FIG. 2. TMA scans of the as-melt-spun and thermally processed $(Nd_{0.95}La_{0.05})_{9.5}Fe_{bal}Co_5Nb_2B_{10.5}$.

RESULTS AND DISCUSSIONS

Shown in Fig. 1 are the variations of B_r, H_{ci}, and BH_{max} obtained with the thermal processing temperatures. H_{ci} increases from 0.1 kOe in the as-spun state to 1.5 kOe when treated at 650 °C, peaks to 11.7 kOe at 700 °C, then decreases to 8.8 and 7.0 kOe when treated at 750 and 850 °C, respectively. Unlike H_{ci}, B_r increases from 1.0 kG in the as-spun state to 4.2, 6.8, and 7.0 kG when treated at 650, 700, and 750 °C, respectively. A slight decrease in B_r (from 7.0 to 6.9 kG) was noticed when treated at 850 °C. It is of interest to note that H_{ci} reaches the highest value at 700 °C, while the highest B_r was obtained when treated at 750 °C. This difference in optimum values may arise from the fact that two different mechanisms: the exchange coupling, and the phase content govern H_{ci} and B_r. While exchange coupling is important for both H_{ci} and B_r, the amount of the soft phase competes with the exchange interaction in its effect on B_r. During this competition, B_r can be increased at the expense of reduced exchange interaction and therefore lowered H_{ci}. At 850 °C, the desired hard and soft magnetic phases may transform into undesired phases and result in the decrease in both H_{ci} and B_r. The trend of BH_{max} is a combined effect of H_{ci} and B_r. BH_{max} begins at 0.0 MG Oe in the as-spun state, reaches a maximum value of 10.1 MG Oe at 700 °C, and then decreases when treated at a temperature higher than 700 °C.

Shown in Fig. 2 are the TMA scans of the samples studied. The as-spun and the 650 °C treated materials show a large amount of the unknown phase with a T_c of 170 °C. The low H_{ci} values obtained on these two samples suggest that this amorphous phase is indeed a soft magnetic phase. During crystallization, this soft and amorphous phase transforms into phases dictated by the nominal alloy composition and the phase transformation paths. Two magnetic phases, namely, $Nd_2(FeCo)_{14}B$ and α-Fe were detected on samples treated at 700 °C. When treated at 750 °C, the amount of α-Fe increased slightly and a traceable amount of Fe_3B was also detected. This increase in the amount of α-Fe is consistent with the slight increase in B_r observed. At 850 °C, the amount of Fe_3B decreased significantly suggesting that Fe_3B may transform into nonmagnetic phases. It should be noted that the T_c of $Nd_2(FeCo)_{14}B$ increased as a function of the thermal processing temperatures. When processed at 650, 700, 750, and 850 °C, the T_c of $Nd_2(FeCo)_{14}B$ was 343, 351, 367, and 395 °C, respectively. This change in T_c may suggest an increased Co content in the $Nd_2(FeCo)_{14}B$ phase.

Shown in Fig. 3(a) are the XRD scans of the samples treated with various thermal processing temperatures. To

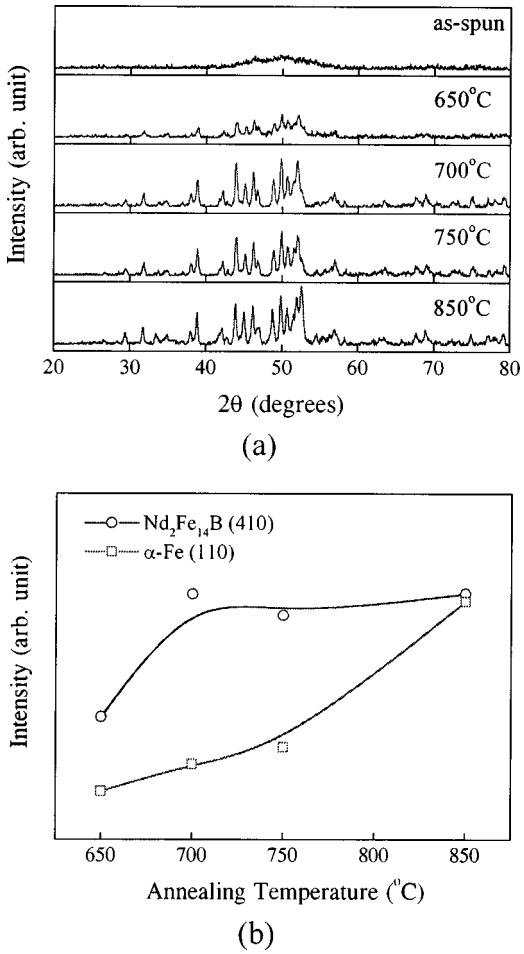

FIG. 3. (a) XRD of as-spun $(Nd_{0.95}La_{0.05})_{9.5}Fe_{bal}Co_5Nb_2B_{10.5}$. (b) Intensities of the (410) peak of $Nd_2(FeCo)_{14}B$ and the (110) peak of α-Fe vs the temperature.

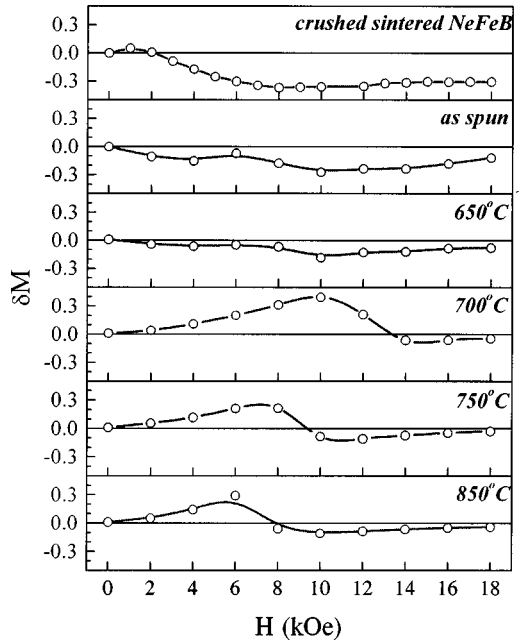

FIG. 4. The Henkel plots of the sintered $Nd_{15}Fe_{79}B_6$ and as-melt-spun and thermally processed $(Nd_{0.95}La_{0.05})_{9.5}Fe_{bal}Co_5Nb_2B_{10.5}$.

compare the growth rate of $Nd_2(FeCo)_{14}B$ and α-Fe, the intensities of the (410) peak of the $Nd_2(FeCo)_{14}B$ phase and the (110) peak of the α-Fe phase were plotted against the temperature in Fig. 3(b). It can be seen that most of the crystallization of the $Nd_2(FeCo)_{14}B$ phase occurred at a temperature lower than 700 °C, while the growth of the α-Fe phase accelerated as the temperature rose.

Shown in Fig. 4 are the Henkel plots, ΔM versus H, of all samples included in this study. To illustrate the effect of grain size on this type of plot, a ΔM versus H curve of a sintered NdFeB with an average grain size of 10 μm, pulverized to an equivalent powder size, was also included for comparison. As expected, the crushed sintered NdFeB showed mostly negative ΔM, suggesting a magnetostatic-dominated particle interaction.[8,9] The ΔM of the as-melt-spun materials and samples heat treated at 650 °C exhibited similar behavior. For samples treated above 650 °C, a positive ΔM was observed indicating the existence of exchange coupling between phases.[1,8,9] The height of the ΔM peak reached a maximum when materials were treated at 700 °C, suggesting that the strongest exchange coupling was among samples studied. At 750 and 850 °C, the peaks of ΔM decreased significantly, an indication of a weakened exchange interaction. Microstructural examinations, both on average grain size and phase distribution, are necessary to quantify this change in exchange coupling.

Listed in Table I are the average grain sizes of the primary and secondary phases determined by the conventional transmission electron microscopy (CTEM) in a supporting article. It suggests that the as-spun materials are fully amorphous. Grains with an average grain size of about 38 nm embedded in a large amount of amorphous residual were observed on samples treated at 650 °C. Material became fully crystallized with an average grain size of 40 nm when treated at 700 °C. The increase in the amount of magnetically hard and soft phases developed in conjunction with the limited increase in the average grain size may explain the highest ΔM peak which occurred at 700 °C. At 750 °C, a slight grain growth occurred and a secondary phase began to precipitate. A bimodel grain size distribution with peaks at 5 and 45 nm was observed. Although the composition of this precipitated phase cannot be accurately identified, these precipitates may be finely dispersed borides. The presence of the secondary phase and the growth of the average grain size of the primary phase from 40 to 45 nm may explain the decrease in ΔM peak from 700 to 750 °C. At 850 °C, the size of the secondary phases grew to 12 nm and the primary phases encountered an excessive growth from 45 to 68 nm. The combination of these two factors and the nonmagnetic nature of the precipitates may be the cause for the decrease in the ΔM peak and the weakened exchange interaction. The growth of these precipitates, in conjunction with the mass balance, may explain the increase in T_c of the $Nd_2(FeCo)_{14}B$ when treated from 650 to 850 °C on the TMA scans. Similarly, this may also explain the slight decrease in the amount of Fe_3B when the thermal processing temperature was increased from 750 to 850 °C.

TABLE I. The average grain sizes obtained via the conventional transmission electron microscopy (CTEM) analysis of the as-spun and thermally processed samples.

Sample	Average grain size (nm) (CTEM)
as-spun	n/a
650 °C	38
700 °C	40
750 °C	5 and 45
850 °C	12 and 68

[1] W. C. Chang, S. H. Wu, B. M. Ma, C. O. Bounds, and S. Y. Yao, J. Appl. Phys. **83**, 2147 (1998).
[2] B. Lu, M. Q. Huang, Q. Chen, B. M. Ma, and D. E. Laughlin, J. Appl. Phys. (these proceedings).
[3] E. F. Kneller and R. Hawig, IEEE Trans. Magn. **27**, 3588 (1991).
[4] R. Skomski and J. M. D. Coey, Phys. Rev. B **48**, 1581 (1993).
[5] T. Schrefl, J. Fidler, and H. Kronmuller, Phys. Rev. B **49**, 6100 (1994).
[6] R. Fischer, T. Schrefl, H. Kronmuller, and J. Fidler, J. Magn. Magn. Mater. **153**, 35 (1996).
[7] J. Ormerod and S. Constantinides, J. Appl. Phys. **81**, 4816 (1997).
[8] E. P. Wohlfarth, J. Appl. Phys. **29**, 595 (1958).
[9] P. E. Kelly, K. O. Grady, P. I. Mayo, and R. W. Chantrell, IEEE Trans. Magn. **25**, 3881 (1989).
[10] M. Fearon, R. W. Chantrell, and E. P. Wohlfarth, J. Magn. Magn. Mater. **86**, 197 (1990).